

# Effect of unevenly-distributed V pits on the optical and electrical characteristics of green micro-light emitting diode

Da-Hoon Lee<sup>1</sup>, Daesung Kang<sup>2</sup>, Tae-Yeon Seong<sup>1,3,5,\*</sup>, Michael Kneissl<sup>4</sup>, and Hiroshi Amano<sup>5</sup>

<sup>1</sup>Department of Nanophotonics, Korea University, Seoul 02841, Korea

<sup>2</sup>LED Division, LG Innotek Co., Ltd., Paju, Gyeonggi 10842, Korea

<sup>3</sup>Department of Materials Science and Engineering, Korea University, Seoul 02841, Korea

<sup>4</sup>Institute of Solid State Physics, Technische Universität Berlin, Hardenbergstr. 36, 10623 Berlin and Ferdinand-Braun-Institut, Leibniz-Institut für Höchstfrequenztechnik, Gustav-Kirchhoff-Str. 4, 12489 Berlin, Germany

<sup>5</sup>for Integrated Research of Future Electronics, and Institute of Materials and Systems for Sustainability, Nagoya University, Nagoya 464-8603, Japan

## ABSTRACT

In this study, we investigated the effect of different-size V pits on the opto-electrical performance of different-size InGaN-based green (520 nm) light-emitting diodes (LEDs). The size of V pits varied from 57 to 250 nm. Two different-size LEDs (10 and 300  $\mu\text{m}$ ) were fabricated with flip-chip structures. It was shown that at 4  $\text{A}/\text{cm}^2$ , the forward voltages of 300  $\mu\text{m}$ -size and 10  $\mu\text{m}$ -size LEDs were in the range of 2.32–2.82 V and 2.23–2.53 V, respectively. Compared with the LEDs with small V pits, the LEDs with large V pits produced higher output power at the high current region ( $> 50 \text{ A}/\text{cm}^2$ ), but lower output power at the low current region ( $< 20 \text{ A}/\text{cm}^2$ ). The 300  $\mu\text{m}$ -size LEDs displayed maximum external quantum efficiency (EQE) at 2  $\text{A}/\text{cm}^2$ , whereas the 10  $\mu\text{m}$ -size LEDs exhibited peak EQE at current densities  $\geq 13 \text{ A}/\text{cm}^2$ . For all samples, the electroluminescence (EL) wavelengths were blue shifted with increasing current density. Unlike the 300  $\mu\text{m}$ -size LEDs, the 10  $\mu\text{m}$ -size LEDs exhibited a large deviation in the light output, EQE, and EL wavelength. The 10  $\mu\text{m}$ -size LEDs revealed larger S than the 300  $\mu\text{m}$ -size LEDs. The backscattered electron (BSE) and monochromatic cathodoluminescence (CL) results showed that for all samples, V pits were unevenly distributed across the whole wafer. Based on the CL and BSE results, the effect of different V pit sizes on the performance of green micro-LEDs at the low current region is described and discussed.

---

\*Corresponding author: E-mail: tyseong@korea.ac.kr (T.-Y. Seong).

## 1. Introduction

The fabrication of high-performance microscale displays is of increasing importance for their applications in augmented reality systems, virtual reality and wearable devices. In this connection, InGaN-based LEDs have been considered as an important light source for self-emissive display [1,2] because of their performance characteristics including performance reliability, high brightness, long lifetime and lower power consumption [3,4]. For example, Day et al. demonstrated GaN-based full scale high-resolution microdisplay fabricated with pixel (chip) dimensions (12  $\mu\text{m}$  in size), which was able to deliver video graphics images [5]. On the one hand, GaN-based LEDs experience the efficiency droop caused by electron overflow [6], nonuniform carrier distribution [7], Auger nonradiative recombination [8] and defect recombination [9] during the operation at high current injection. It was found that such efficiency droop might be alleviated by reducing chip size, namely, adopting micro-LEDs [10]. Different shapes of micro-LEDs, including microdisk [11], microring [12] or conventional rectangular chips [4,13], have been investigated. As compared with conventional large LEDs, micro-LEDs presented better thermal behavior [13] and light extraction [14], and operation at higher current densities [15]. However, these merits notwithstanding, surface recombination at the sidewalls of micro-LEDs was found to play a key role in lowering the quantum efficiencies of chips [16–19]. For instance, it was reported that as the chip size increased from 60 to 160  $\mu\text{m}$  in diameter, the current density decreased at the same forward voltage, while the light output increased at the same current density and their EQE peaks were attained at lower current densities. These output power characteristics were attributed to the mutual effects of increasing nonradiative recombination, carrier leakage and self-heating effect [16]. It was also observed that smaller LED experienced less shift in the electroluminescence (EL) spectra as compared

with larger chips [18]. Moreover, with increasing current density, larger chips underwent faster junction temperature rise than smaller chips.

Furthermore, it was observed that the quantum efficiency of InGaN-based LEDs was directly affected by the formation of V pits in the QWs [13,20–24]. It was reported that V pits are formed at the dislocation surface termination [21]. The size of V pits was shown to be controlled by changing either the thickness of a low temperature GaN buffer or the number of low-temperature InGaN/GaN interfaces [21,23]. It was also found that the internal quantum efficiency (IQE) of green LEDs increased as the V-pit size increased from 100 to 220 nm, above which the IQE decreased [23]. The improvement associated with V pits was ascribed to the combined effects of large potential barriers at V pits, the loss of MQW region and increase in the compressive stress in LEDs [21–23]. Thus, considering the importance of V pits, the investigation of their effects on the optical performance of micro-scale LEDs is imperatively needed. Besides, since V pits are directly related to threading dislocations (TDs) [21], V pits are not uniformly distributed across the whole wafer. Thus, unlike large-size LEDs (e.g., > 300  $\mu\text{m}$ ), each small-size chip (e.g., micro-LEDs < 20  $\mu\text{m}$ ) could contain different numbers of V pits, depending on its location in the wafer. This can cause a variation in the performance of micro-LEDs of the same wafer. To the best of our knowledge, however, such behavior has not been hitherto characterized. Thus, in this study, we examined the electrical and optical properties of green (520 nm) GaN-based micro-LEDs as a function of the LED size and distribution of V pits, whose size varied from 57 to 250 nm. Cathodoluminescence (CL) and EL examinations were made to evaluate the defect behaviour and recombination efficiency, respectively. To investigate the defect features of LEDs with different-size V pits, we examined S value, which is given by  $\partial \ln L / \partial \ln I$  [25], where  $I$  is the current density, and  $L = \eta_c B N^2$  is the light output power,  $\eta_c$  is the coupling efficiency,  $B$  is the radiative recombination coefficient,

and  $N$  is the carrier concentration in the MQW region. It should be stressed that in this study, for each of six different types of LEDs, 12 LED chips were assessed to characterise the typical electrical and optical properties.

## 2. Experimental procedures

Green (520 nm) InGaN/GaN-based multiple quantum-well (MQW) LED structures were grown on (0001) sapphire substrates using metalorganic chemical vapor deposition. The LED structure consisted of 0.15  $\mu\text{m}$ -thick Mg-doped  $p$ -type GaN, 20 nm-thick AlGaIn electron blocking layer, 9 pairs of InGaN/GaN MQW, 70 nm-thick strained layer superlattice, 4  $\mu\text{m}$ -thick Si-doped  $n$ -type GaN, and 2  $\mu\text{m}$ -thick undoped GaN on a substrate. At 800 °C, a GaN buffer layer (MT-GaN) was grown on  $n$ -GaN to create V pits [23]. Three different sizes of V pits were produced by controlling the thickness of MT-GaN. In other words, the growth of 55 nm-, 110 nm-, and 220 nm-thick MT-GaN resulted in the generation of V pits with size of 57, 105 and 250 nm, respectively (which are referred to here as ‘small V pit’, ‘mid V pit’, and ‘large V pit’). The density of V pits was estimated to be  $2 \times 10^8 \text{ cm}^{-2}$ . After growth, two different-size LEDs (10 and 300  $\mu\text{m}$ ) with three different V pit sizes were fabricated with flip-chip structures, which were referred to here as 10  $\mu\text{m}$ -size and 300  $\mu\text{m}$ -size LEDs, respectively. To form  $p$ -type reflective Ohmic contact, a Ni (3 nm)/Ag (200 nm)/Ni (50 nm) layer was deposited by electron beam evaporation, followed by annealing at 500 °C for 5 min in air. To form  $n$ -type Ohmic electrode, a Cr (10 nm)/Al (200 nm)/Ni (50 nm)/Au (50 nm) layer was deposited. A high-current source-measuring unit (Keithley 2602) was employed to measure current-voltage ( $I$ - $V$ ) characteristics. Electroluminescence (EL) and output powers were examined to characterise the performance of micro-LEDs containing different numbers of V pits by means of an Ocean optics (USB2000) and a Newport dual-channel power meter,

respectively. Scanning electron microscopy (SEM) (TESCAN) coupled to a CL system (Sparc, Delmic, Holland) was used to investigate the surface and defect properties, respectively.

### 3. Results and discussion

Fig. 1 exhibits the forward voltage characteristics of two different size LEDs with various V pits as a function of current density, which were the average values obtained from 12 different devices. It is found that the 300  $\mu\text{m}$ -size LEDs gave higher forward voltage than the 10  $\mu\text{m}$ -size LEDs across the whole current region. For instance, the forward voltages of the 300  $\mu\text{m}$ -size LEDs were in the range of 2.32–2.82 V at 4 A/cm<sup>2</sup>, whereas those of the 10  $\mu\text{m}$ -size LEDs ranged from 2.23 to 2.53 V. The better forward voltage characteristics of the 10  $\mu\text{m}$ -size LEDs can be ascribed to the better current spreading and injection [16,26–28]. In addition, regardless of the chip size, the forward voltage of LEDs decreased with increasing V-pit size. This can be explained as follows. It was reported that the existence of V pits not only increased the hole injection into the QWs but also enhanced the uniformity of the hole density distribution in QWs [29]. It was found that the potential barrier formed by V pits increased with increasing V-pit size up to 250 nm [23]. Consequently, the forward voltage of LEDs decreased with an increase in the size of V pits. It is noted that the 10  $\mu\text{m}$ -size LEDs revealed a larger deviation in the forward voltage than the 300  $\mu\text{m}$ -size LEDs. This is particularly true for the one with mid V pits. This size dependence is consistent with the previous results presented by other groups [16,26–28].

Fig. 2 reveals the typical output power-current density ( $L$ - $I$ ) relations for different size LEDs as a function of V pit size, which were the average values obtained from 12 different devices. It is shown that irrespective of chip and V pit sizes, the output power increased with an increase in the current density. It is noted that the samples with larger V pits produced higher output

than small ones at the high current region ( $> 50 \text{ A/cm}^2$ ). This is consistent with the findings reported by other groups [21–23], where LEDs with large V pits (e.g., 180–215 nm in diameter) yielded higher IQE than those with small V pits (e.g., 100 nm). However, at the low current region ( $< 20 \text{ A/cm}^2$ ), at which micro-LEDs for display are operated, the  $L-I$  curves show different output characteristics, as shown in Fig. 3. It should be noted that the  $L-I$  curves were the average values obtained from 12 different devices. For both of the chip sizes, LEDs containing small V pits exhibited the highest output power. This is different from the results obtained in the high current region ( $> 50 \text{ A/cm}^2$ ). Furthermore, regardless of the V pit size, the 300  $\mu\text{m}$ -size LEDs exhibited higher light output at the same current density than the 10  $\mu\text{m}$ -size LEDs [28]. This can be related to combination of the larger emission area and a reduction in the Shockley-Read-Hall (SRH) nonradiative recombination [30] induced by dry-etching [16,27,28]. It was reported that V pits could cause efficient hole injection and screening of TDs due to the large potential barrier [21–23], improving LED performance. On the other hand, V pits were also known to bring about the area loss of MQWs. For example, the surface coverage ratios of the V pits in green MQWs with 100 and 215 nm-size V pits were approximately 1.2 and 4.0%, respectively [23]. Thus, at the low currents, optimal V pit size may play a dominant role in improving the output power, namely, the smaller V pit the larger output. Notably, the 10  $\mu\text{m}$ -size LEDs display larger scatter in the output powers than the 300  $\mu\text{m}$ -size LEDs. The deviation increased with increasing V pit size and current density.

Relation between relative EQE and LED size is illustrated in Fig. 4, which were the average values obtained from 12 different devices. Note that relative EQEs were used in this study because it is difficult to handle micro-LEDs ( $< 50 \mu\text{m}$ ) in packaging process. It is noteworthy that the 300  $\mu\text{m}$ -size LEDs displayed peak EQE at  $2 \text{ A/cm}^2$ , whereas the 10  $\mu\text{m}$ -size LEDs exhibited a peak EQE at higher currents. For instance, the peak EQE for the 10  $\mu\text{m}$ -size LEDs

was attained at 13, 19 and 20 A/cm<sup>2</sup> for the small, mid, and large V pits, respectively. Note that the sidewall to surface ratios for the 10 μm- and 300 μm-size LEDs were calculated to be 0.048 and 0.0016, respectively. Thus, the attainment of the peak EQE at higher currents could be associated with SRH nonradiative recombination or leakage current due to sidewall defects [16,27,28]. Currently, the reason why different V pit size exhibited different peak EQEs is not evidently understood. However, this might be related to the fact that large V pits could be cut by the edge of 10 μm-size LEDs, producing more defect areas. It was further observed that unlike the 300 μm-size LEDs, the 10 μm-size LEDs experienced less obvious efficiency droop. This could be because different from the 300 μm-size LEDs, the 10 μm-size LEDs had lower maximum EQEs because of SRH nonradiative recombination, which was followed by Auger recombination [30] giving low EQE. It is worthwhile to note that the 10 μm-size LEDs illustrated larger deviation in the EQE than the 300 μm-size LEDs.

EL spectra of different-size LEDs containing three different-size V pits were examined as a function of current density. It was observed that the EL intensity of all samples increased with increasing current density to 20 A/cm<sup>2</sup>. Fig. 5 illustrates the EL wavelength for LEDs as a function of the size of V pits, which were the average values obtained from 12 different devices. There are three distinctive features. First, for all samples, their peak wavelengths were blue shifted as the current increased. This shift can be attributed to the screening of the quantum confined Stark effect and/or band-filling effect [23,31]. In particular, the LEDs with larger V pits exhibited larger blue shift than the ones with small V pits. This is in agreement with the previous results, showing that the larger V pits caused more efficient current injection and effective screening of QCSE, resulting in larger blue shift [32]. Second, unlike the 300 μm-size LEDs, the 10 μm-size LEDs exhibited a large deviation in the EL wavelength. This feature becomes less pronounced with a decrease in the size of V pits. The exact mechanism why the

10  $\mu\text{m}$ -size LED with large V pits exhibited larger deviation than the others is not clearly understood. However, the mechanism may be described as follows. The presence of V pits geometrically reduces the total c-plane area of MQW region and so the total area of MQW region decreases with increasing V pit size. Thus, at the same current density, the actual current density per unit area increases as the V pit size increases. This feature is similar to the phenomenon where the EL wavelength decreases with increasing current density. Consequently, the deviation occurs because of the inhomogeneous distribution of V pits within the 10  $\mu\text{m}$ -size LED wafers and is more severe in the large V pits than smaller ones. The results indicate that the variation in the EL wavelength of the 10  $\mu\text{m}$ -size LEDs can be minimized by reducing the size of V pits. Third, regardless of chip sizes, the EL peak wavelength at a low current of 4  $\text{A}/\text{cm}^2$  was blue shifted with a decrease in the V pit size. For example, as the V pit size decreased from 250 nm to 57 nm, the wavelength of the 300  $\mu\text{m}$ -size LEDs varied from 517.9 nm to 510.5 nm. This V pit size dependence of the wavelength could be caused by the different growth conditions of the MT-GaN used to form different V pit sizes, e.g., a fluctuation of the temperatures for different growth runs for the MT-GaN layers. Consequently, this may cause a change in the indium content in the QWs, thereby resulting in a variation in the EL wavelengths.

Fig. 6 demonstrates the current density dependence of S values for the various LEDs, which were the average values obtained from 12 different devices. The S is expected to be 2.0 for dominant SRH recombination [25,26,31]. It is noted that the 10  $\mu\text{m}$ -size LEDs showed larger S than the 300  $\mu\text{m}$ -size LEDs. This illustrates dominant SRH recombination in the 10  $\mu\text{m}$ -size LEDs. In addition, the S converged to 1.0 as the current density increased to 20  $\text{A}/\text{cm}^2$ . For all samples, the S decreased with increasing V pit size. This is more obvious for the 10  $\mu\text{m}$ -size LEDs. The S value of 1.0 denotes radiative recombination, while that  $< 1.0$  represents carrier

overflow or Auger recombination [26,29,31].

The electrical and optical results showed that the 10  $\mu\text{m}$ -size LEDs displayed larger deviation in the light output, EQE and wavelength compared with the 300  $\mu\text{m}$ -size LEDs. These different electrical and optical characteristics could be related to the materials property, namely, the presence of different sizes of V pits. Thus, to directly investigate the distribution of V pits, backscattered electron (BSE) and monochromatic CL images from LED wafers with different sizes of V pits were examined, as shown in Fig. 7. For all samples, the BSE images exhibit numerous small dark spots, which correspond to V pit defects (Figs. 7(a), 7(c), and 7(e)). The CL images show that for all samples, regions ( $120 \times 90 \mu\text{m}^2$ ) from the LED wafers reveal overall non-uniform intensity distribution (Figs. 7(b), 7(d), and 7(f)), implying a large variation in the number of V pits across the whole wafers. This means that unlike the large area ( $300 \times 300 \mu\text{m}^2$ ), there must be a wide range of variation in the V pit density in the micro-regions ( $10 \times 10 \mu\text{m}^2$ ) from the same wafers (Figs. 7(b), 7(d), and 7(f)). Therefore, since the existence of V pits directly improves LED performance of [21–23], the large variation in the micro-LED performance can be ascribed to the uneven distribution of V pits, as demonstrated in the CL images (Figs. 7(b), 7(d), and 7(f)). The distribution of different-size V pits that was obtained from ten random areas ( $63 \mu\text{m}^2$ ) across the wafer is illustrated in Fig. 8. This clearly displays a variation of V pits across the wafer. It is found that about 40% of the areas contain 80 – 100 V pits/ $\mu\text{m}^2$ . This shows that it is very important not only to optimise the size of V pits but also to reduce the density of TDs for fabricating high-efficiency micro-LEDs with uniform electrical and optical performance.

#### 4. Conclusions

We investigated how the distribution of different V pit sizes affected the EQE and EL of InGaN-based green LEDs were characterized. The 10  $\mu\text{m}$ -size LEDs had smaller forward voltages than the 300  $\mu\text{m}$ -size LEDs across the current density up to 20  $\text{A}/\text{cm}^2$ . The LEDs with large V pits demonstrated higher light output at high current region, but lower output at low current region than the LEDs with small V pits. The 300  $\mu\text{m}$ -size LEDs reached peak EQE at lower current than the 10  $\mu\text{m}$ -size LEDs. The EL wavelengths were blue shifted with increasing current density. Unlike the 300  $\mu\text{m}$ -size LEDs, the 10  $\mu\text{m}$ -size LEDs exhibited a large deviation in the light output, EQE, and EL wavelength. The 10  $\mu\text{m}$ -size LEDs revealed larger S than the 300  $\mu\text{m}$ -size LEDs. The BSE and CL results exhibited the uneven distribution of V pits across the whole wafer. These results indicate that the growth of the optimal size of V pits and the reduction in TD density are crucial for realizing the uniform electrical and optical performance of high-efficiency micro-LEDs.

## Acknowledgments

This work was supported by the Global Research Laboratory (GRL) program through the National Research Foundation (NRF) of Korea (NRF-2017K1A1A2013160).

## References

1. C.-J. Chen, H.-C. Chen, J.-H. Liao, C.-J. Yu, M.-Ch. Wu, *IEEE J. Quantum Electron.* **55**(2), 3300106 (2019).
2. Y. Fu, J. Sun, Z. Du, W. Guo, C. Yan, F. Xiong, L. Wang, Y. Dong, C. Xu, J. Deng, T. Guo, Q. Yan, *Mater.* **12**(3), 428 (2019).
3. T. Tao, T. Zhi, X. Cen, B. Liu, Q. Wang, Z. Xie, P. Chen, D. Chen, Y. Zhou, Y. Zheng, *IEEE Photon. Journal* **10**(5), 8201608 (2018).
4. J.-T. Oh, Y.-T. Moon, J.-H. Jang, J.-H. Eum, Y.-J. Sung, S. Y. Lee, J.-O Song, and T.-Y.

- Seong, J. Alloy. Comp. **732**, 630 (2018).
5. J. Day, J. Li, D.Y.C. Lie, C. Bradford, J.Y. Lin, and H.X. Jiang, Appl. Phys. Lett. **99**(3), 031116 (2011).
  6. P. Prajoun, M.A. Menokey, J. Charles Pravin, J. Ajayan, S. Rajesh, D. Nirmal, Superlatt. Microstruc. **116**, 71 (2018).
  7. A. David, M. J. Grundmann, J. F. Kaeding, N. F. Gardner, T. G. Mihopoulos, and M. R. Krames, Appl. Phys. Lett. **92**(5), 053502 (2008).
  8. E. Kioupakis, P. Rinke, K. T. Delaney, and C. G. Van de Walle, Appl. Phys. Lett. **98**(16), 161107 (2011).
  9. B. Monemar and B. E. Sernelius, Appl. Phys. Lett. **91**(18), 181103 (2007).
  10. S.-C. Huang, H. Li, Z.-H. Zhang, H. Chen, S.-C. Wang, and T.-C. Lu, Appl. Phys. Lett. **110**(2), 021108 (2017).
  11. L. Dai, B. Zhang, J. Y. Lin, and H. X. Jiang, J. Appl. Phys. **89**(9), 4951 (2001).
  12. H. W. Choi, M. D. Dawson, P. R. Edwards, and R. W. Martin, Appl. Phys. Lett. **83**(22), 4483 (2003).
  13. D.-H. Kim, Y.S. Park, D. Kang, K.-K. Kim, T.-Y. Seong, H. Amano, J. Alloy. Comp. **796**, 146 (2019).
  14. H. W. Choi, C. W. Jeon, M. D. Dawson, P. R. Edwards, R. W. Martin, and S. Tripathy, J. Appl. Phys. **93**(10), 5978 (2003).
  15. S. Lu, W. Liu, Z.H. Zhang, S.T. Tan, Z. Ju, Y. Ji, X. Zhang, Y. Zhang, B. Zhu, Z. Kyaw, N. Hasanov, X.W. Sun, and H.V. Demir, Opt. Express **22**(26), 32200 (2014).
  16. H. Huang, H. Wu, C. Huang, Z. Chen, C. Wang, Z. Yang, H. Wang, Phys. Status Solidi A **215**(24), 1800484 (2018).
  17. M. Peng, X. Zheng, S. Liu, H. Wei, Y. He, M. Li, Y. An, Y. Song, P. Qiu, Nanoscale **11**(8), 3710 (2019).
  18. Z. Gong, S. Jin, Y. Chen, J. McKendry, D. Massoubre, I. M. Watson, E. Gu, M. D. Dawson, J. Appl. Phys. **107**(1), 013103 (2010).
  19. B. Alhalaili, D.M. Dryden, R. Vidu, S. Ghandiparsi, H. Cansizoglu, Y. Gao, M.S. Isalm, Appl. Nanosci. **8**(5), 1171 (2018).
  20. Z. Quan, J. Liu, F. Fang, G. Wang, F. Jiang, J. Appl. Phys. **118**(19), 193102 (2015).
  21. N. Okada, H. Kashihara, K. Sugimoto, Y. Yamada, and K. Tadatomo, J. Appl. Phys. **117**(2), 025708 (2015).

22. C.-Y. Chang, H. Li, Y.-T. Shih, and T.-C. Lu, *Appl. Phys. Lett.* **106**(9), 091104 (2015).
23. S. Zhou, X. Liu, H. Yan, Y. Gao, H. Xu, J. Zhao, Z. Quan, C. Gui and S. Liu, *Sci. Rep.* **8**, 11053 (2018).
24. A. Bag, S. Das, R. Kumar, D. Biswas, *CrystEngComm* **20**(29), 4151 (2018).
25. D.P. Han, C.H. Oh, D.G. Zheng, H.Kim, J.I. Shim, K.S. Kim, and D.S. Shin, *Jpn. J. Appl. Phys.* **54**(2S), 02BA01 (2015).
26. J.-T. Oh, S.-Y. Lee, Y.-T. Moon, J. H. Moon, S. Park, K. Y. Hong, K. Y. Song, C.-H. Oh, J.-I. Shim, H.-H. Jeong, J.-O Song, H. Amano, T.-Y. Seong, *Opt. Express* **26**(9), 11194 (2018).
27. F. Olivier, A. Daami, C. Licitra, F. Templier, *Appl. Phys. Lett.* **111**(2), 022104 (2017).
28. D.-H. Kim, Y.-S. Park, D. Kang, K.-K. Kim, T.-Y. Seong, H. Amano, *J. Alloys Comp.* **796**, 146 (2019).
29. Z. Quan, L. Wang, C. Zheng, J. Liu, *J. Appl. Phys.* **116**(18), A779–A789 (2014).
30. D.P. Han, D.G. Zheng, C.H. Oh, H. Kim, J.I. Shim, D.S. Shin, K.S. Kim, *Appl. Phys. Lett.* **104**(15), 151108 (2014).
31. K. Lee, S. Chae, J. Jang, D. Min, J. Kim, D. Eom, Y.-S. Yoo, Y.-H. Cho, O. Nam, *Nanotechnol.* **26**, 335601 (2015).
32. Y. Zhao, S. H. Oh, F. Wu, Y. Kawaguchi, S. Tanaka, K. Fujito, J. S. Speck, S. P. DenBaars, and S. Nakamura, *Appl. Phys. Express* **6**(6), 062102 (2013).

## Figure captions

Fig. 1. The forward voltage characteristics of two different size LEDs with various V pits as a function of current density.

Fig. 2. The output power-current density ( $L-I$ ) curves for (a) 300  $\mu\text{m}$ -and (b) 10  $\mu\text{m}$ -size LEDs as a function of V pit size.

Fig. 3. The output power of (a) 300  $\mu\text{m}$ -and (b) 10  $\mu\text{m}$ -size LEDs with different V pit size in the low current region ( $< 20 \text{ A/cm}^2$ ).

Fig. 4. The dependence of relative external quantum efficiency (EQE) on the LED sizes.

Fig. 5. EL wavelengths for (a) 300  $\mu\text{m}$ -and (b) 10  $\mu\text{m}$ -size LEDs as a function of the size of V pits.

Fig. 6. The current density dependence of S for different samples as a function of the size of V pits.

Fig. 7. (a), (c), and (e) BSE and (b), (d), and (f) monochromatic CL images obtained from LED wafers with the V pit size of 250, 105, and 57 nm, respectively.

Fig. 8. Distribution of different-size V pits, which was obtained from ten random areas ( $63 \mu\text{m}^2$ ) across the wafer.

Figure 1

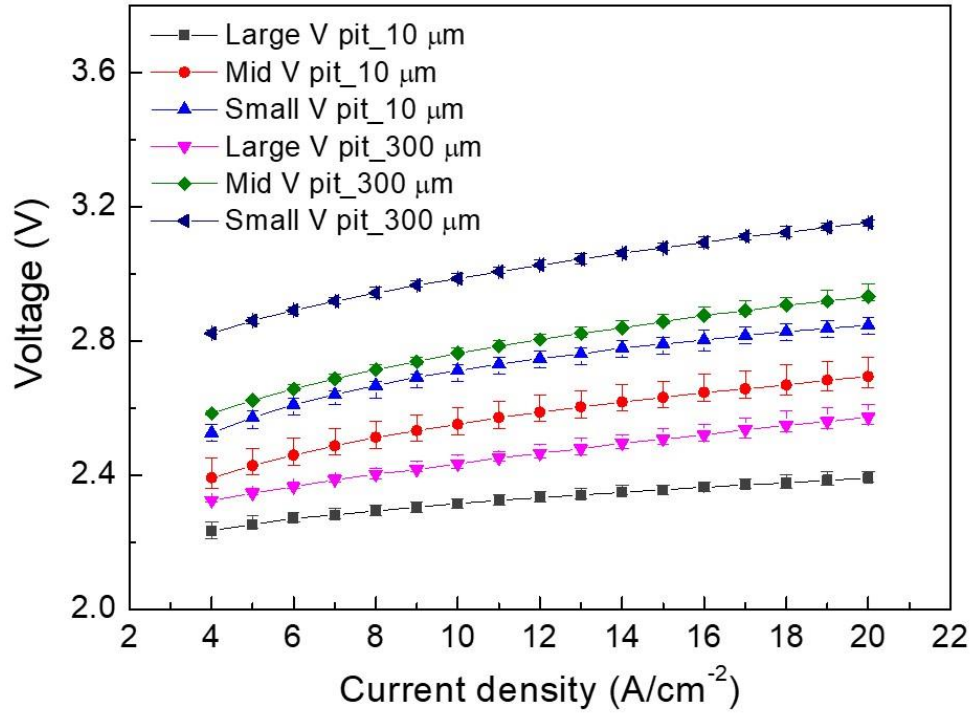


Figure 2

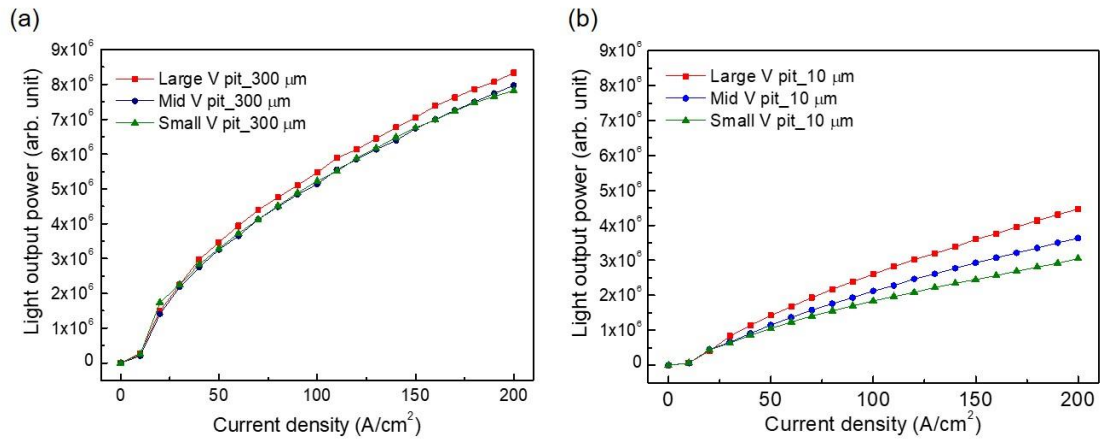


Figure 3

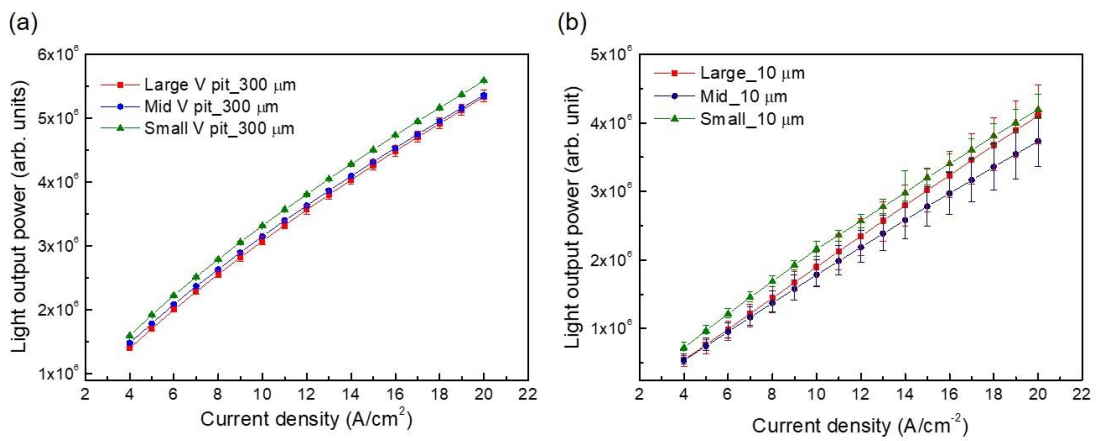


Figure 4

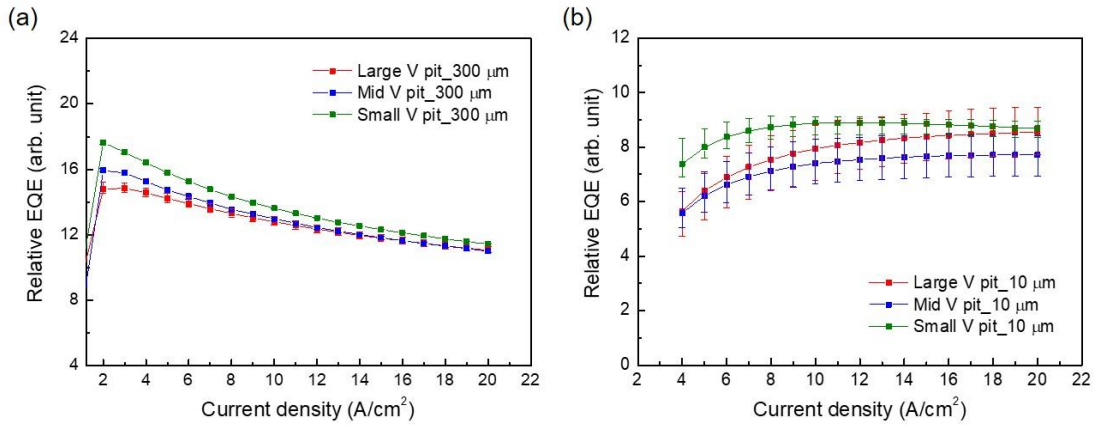


Figure 5

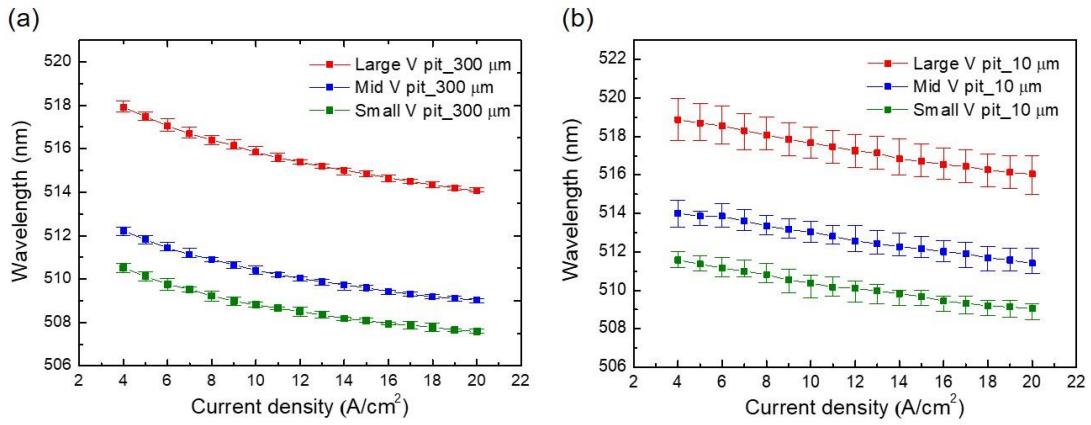


Figure 6

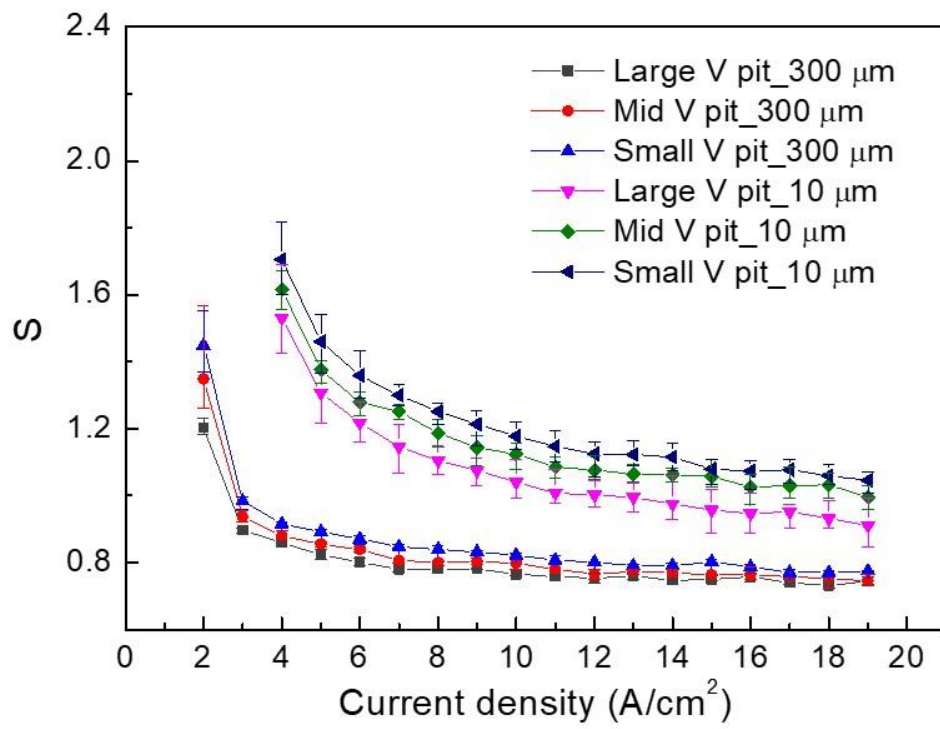


Figure 7

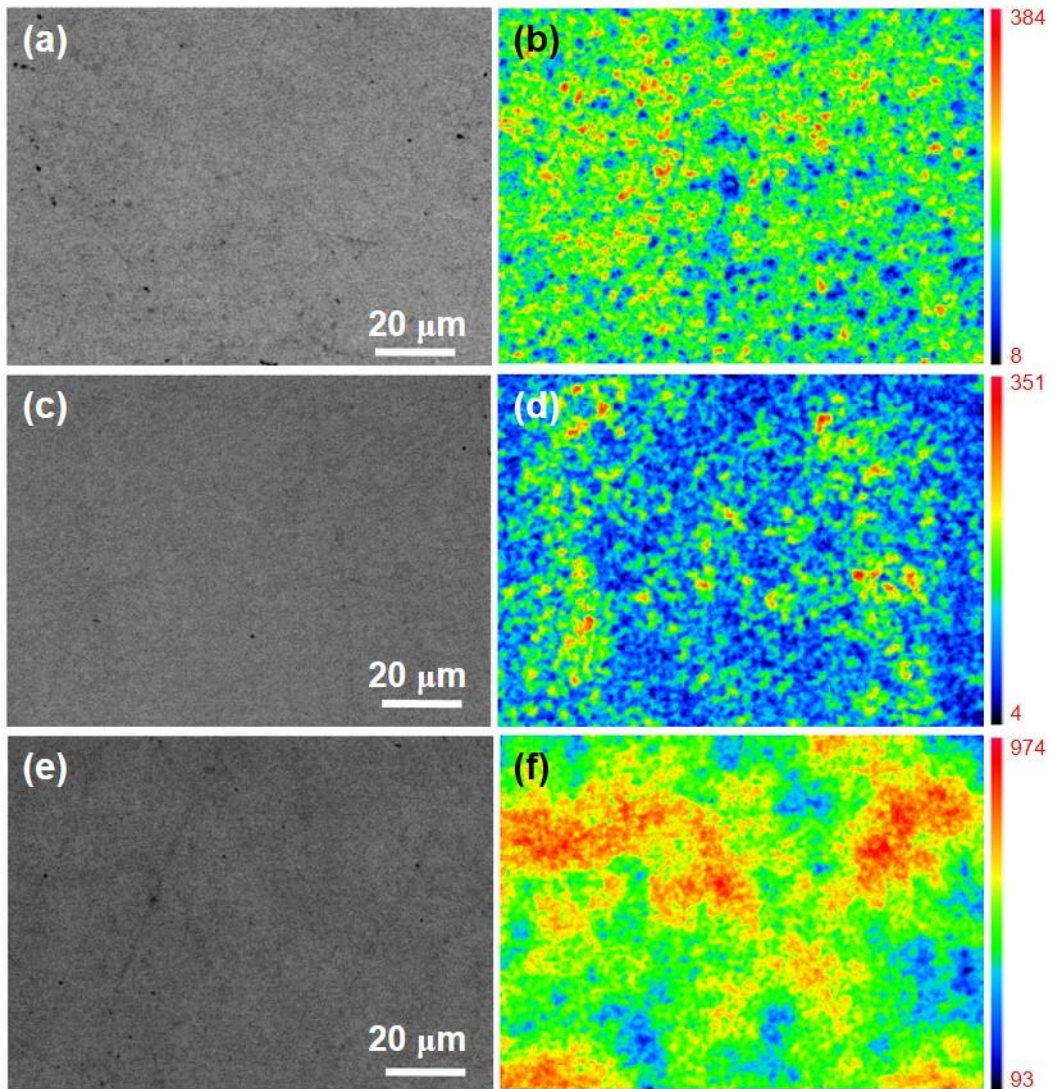


Figure 8

